Supporting Information

Surface modification of alumina-coated silica nanoparticles in aqueous sols with phosphonic acids and impact on nanoparticle interactions

Céline Schmitt Pauly[1,2], Anne-Caroline Genix[2], Johan G. Alauzun[1], Michael Sztucki[3], Julian Oberdisse[2,4], P. Hubert Mutin[1]

[1] *Institut Charles Gerhardt Montpellier, UMR 5253, CNRS-UM-ENSCM, Université de Montpellier, Place Eugène Bataillon, CC1701, F-34095 Montpellier Cedex 5, France*

[2] *Laboratoire Charles Coulomb (L2C), UMR 5221 CNRS-Université de Montpellier, F-34095 Montpellier, France.*

[3] *ESRF - The European Synchrotron, 71 av des Martyrs, CS40220, F-38043 Grenoble, France*

[4] *Laboratoire Léon Brillouin, UMR 12 CNRS/CEA, CEA Saclay, F-91191 Gif sur Yvette, France*

This document gives details regarding the synthesis of PA with short alkyl groups, the NP size, and complementary data related to IR, TGA, and small-angle scattering.

1. Synthesis of C_3PA and C_5PA

Propylphosphonic and pentylphosphonic acids were synthesized in the following way.

49.8 g (0.3 mol) of triethylphosphite was gradually added via syringe into a flask containing 0.24 mol of 3-bromopropane (29.5 g) or 5-bromopentane (36.2 g), which was attached to a reflux condenser, a bubbler, and a septum. After thorough mixing, the reaction was refluxed for 12 h in a 150 – 160°C oil bath under argon to continuously remove the bromoethane away. After the cooling, the reaction mixture was distilled under reduced pressure (0.05 mbar) to give 23.8 g (55%) of pure diethylpropylphosphonate or 26.5 g (53%) of pure diethylpentylphosphonate.

Diethylpropylphosphonate (22.5 g, 0.125 mol) or diethylpentylphosphonate (26.0 g, 0.125 mol) were then placed into a flask equipped with a reflux condenser and containing 40 mL of dry CH_2Cl_2 under an argon atmosphere. 57.4 g (0.375 mol) of Me_3SiBr were then added via syringe and the reaction mixture was stirred for 3 hours at room temperature. The solution was then concentrated under vacuum and 1.875 mol (33.75 mL) of HPLC grade water was added dropwise under an argon atmosphere. The reaction mixture is then stirred for 12 hours, concentrated in vacuum and the crude oily white solid recristallized from hot acetonitrile to obtain 13.8 g (89%) of propylphosphonic acid or 15.05 g (79%) of pentylphosphonic acid.

2. Characterization of the nanoparticles

The form factor of Levasil nanoparticles measured by SAXS is shown in Fig. S1.

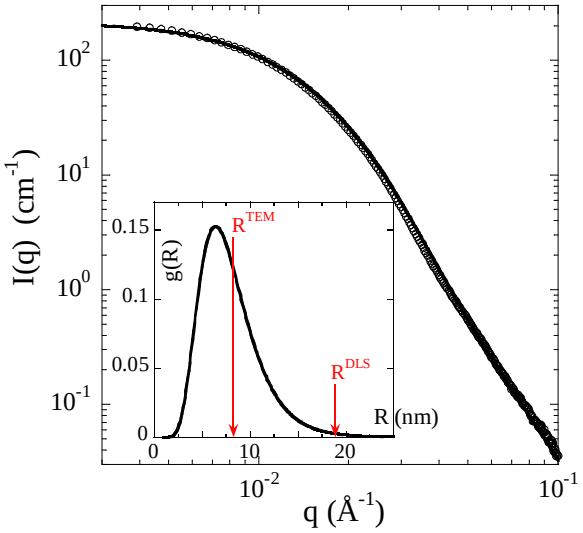

Fig. S1 Scattered intensity I(q) of colloidal alumina-coated silica at 0.2 vol % in water. The line is the description by the form factor of spheres taking into account a log-normal poydispersity. Inset: normalized NPs size distribution g(R) obtained by fitting to the form factor [1]. Arrows indicate the characteristic radii from TEM and DLS.

The different characterizations and properties of the nanoparticles are summarized in Table 1 in the article. The density of NPs was determined by helium pycnometry with a Micromeritics AccuPyc 1330 apparatus. The specific surface area of NPs was determined by nitrogen physisorption at 77 K on a Micromeritics Tristar sorptometer. Prior to analysis, the dried

nanoparticles were degassed under vacuum (2 Pa) at 150°C overnight. The specific surface area was determined via the BET method [2], assuming an area of 0.162 nm^2 per N_2 molecule.

HLB values of the different PA grafts are summarized in Table S1.

Table S1 Phosphonic acid molecules used for grafting alumina-silica NPs.

Phosphonic acid	Notation	HLB [3, 4]
$H_3C(CH_2)_7PO(OH)_2$	C_8PA	16.5
$H_3C(CH_2)_4PO(OH)_2$	C_5PA	17.9
$H_3C(CH_2)_2PO(OH)_2$	C_3PA	18.9
$HOOC(CH_2)_5PO(OH)_2$	CAPA	20.0
$H(OCH_2CH_2)_3PO(OH)_2$	DEPA	21.9

3. Infrared spectroscopy (IR)

Fig. S2 shows the FTIR spectra of the modified NPs. In Fig. S2(a), the vibrations in the 1000-1300 cm^{-1} range can be ascribed to the antisymmetric Si-OM (M = Si or Al) stretching, the shoulder at ca 950 cm^{-1} to Si-OH (possibly Al-OH) antisymmetric stretching. The sharp vibration at 810 cm^{-1} is ascribed to the symmetric Si-OM (M = Si or possibly Al) stretching (used for the normalization of the spectra).

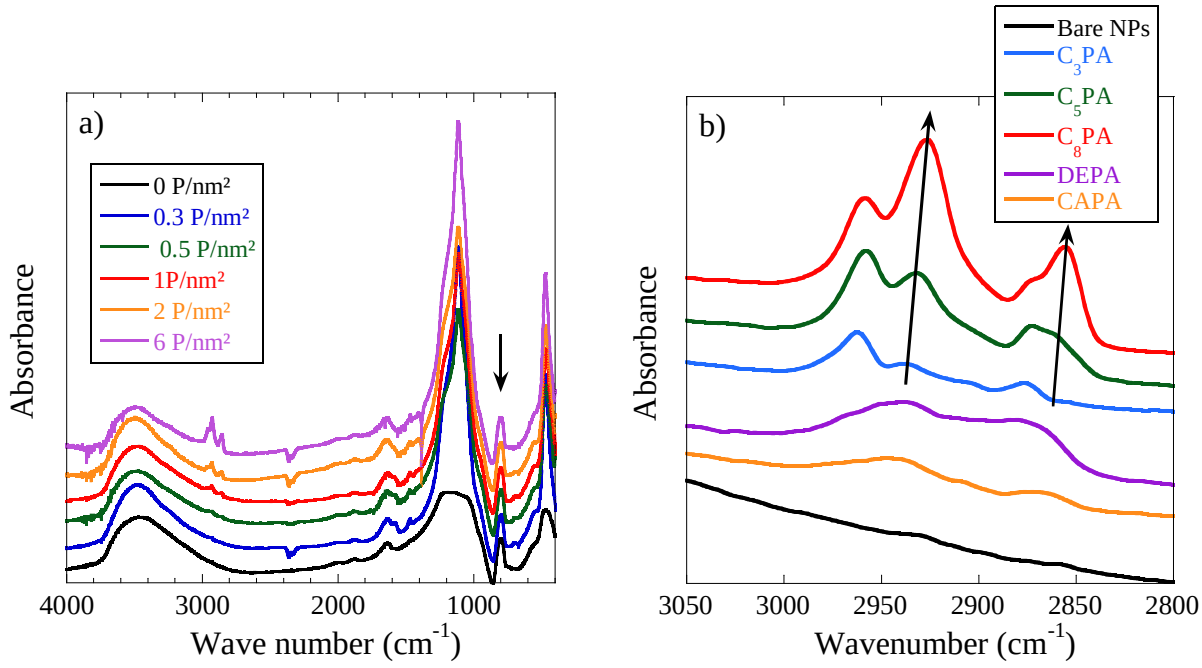

Fig. S2 (a) FTIR spectra of NPs grafted with C_8PA at nominal grafting densities between ρ_{nom} = 0 (bare) and 6 P/nm^2. The arrow indicates the band used for normalization. (b) FTIR spectra of the C-H stretching region of the bare NPs and NPs grafted with the different PAs (ρ_{nom} = 4 P/nm^2). Spectra are shifted vertically for clarity.

Fig. S2(b) shows the vibrations associated to the C-H stretching of the methyl and methylene groups. The asymmetric CH_2 stretching at 2937 cm^{-1} in C_3Pa is shifted to lower wavenumber values when increasing the length of the alkyl group (2926 cm^{-1} in C_8Pa). These values suggest that the monolayers are rather disordered, with order increasing with the alkyl chain length. The same trend is observed in self-assembled monolayers of long-chains alkylphosphonic acids [5]. Note that such an effect is also discernable on the symmetric CH_2 stretching vibrations around 2860 cm^{-1} (see arrows in Fig. S2(b)).

4. Thermogravimetric analysis (TGA)

TGA was performed under air (flow: 50 mL/min) from 20 to 800°C with a heating rate of 5°C/min on a Netzsch STA 409 PC Luxx thermoanalyzer. The average of three different TGA runs of raw NP powders dried before at 120°C gave a weight loss of 4.7% between 200°C and 800°C, which is attributed to the condensation of hydroxyl groups.

The TGA curves of bare and modified NPs provide evidence of the grafting (Fig. S3).

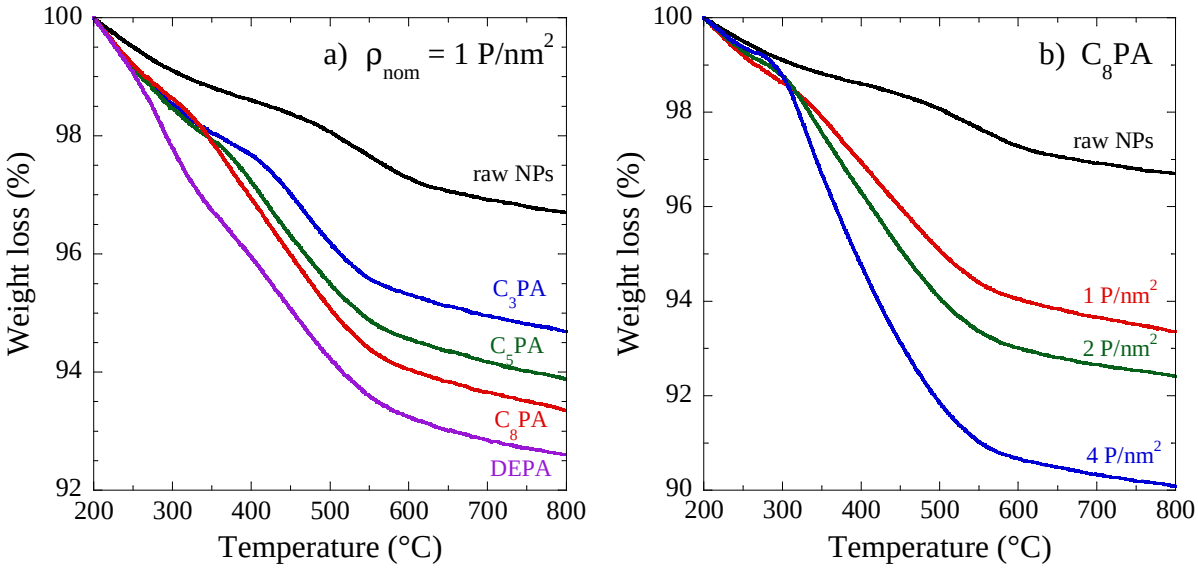

Fig. S3 TGA curves for the modified and bare NPs. (a) Grafting with various phosphonic acids with nominal grafting density ρ_{nom} = 1 P/nm^2. (b) Grafting with C_8PA, ρ_{nom} = 0 – 4 P/nm^2.

The weight losses are given in Table S2.

Table S2 Weight loss between 200 and 800°C in air for the different NPs investigated.

PA	**Nominal ρ (P/nm^2)**	**ΔM/M**
Bare NPs	0	3.3 %
C_3PA	1.0	5.3 %
C_5PA	1.0	6.1 %
C_8PA	1.0	6.6 %
C_8PA	2.0	7.6 %
C_8PA	3.9	9.9 %
DEPA	1.1	7.4 %
DEPA	1.9	9.0 %
DEPA	5.3	14.8 %

5. ICP-OES

The nominal grafting densities of the modified NPs are given in Table S3, where they are compared to the values measured using ICP-OES.

Table S3 Nominal and measured grafting density for the modified NPs. The nominal values are corrected for the PA water content.

PA	Nominal ρ (P/nm^2)	Measured ρ (P/nm^2)
C_3PA	0.47	0.40
C_3PA	0.96	0.93
C_3PA	4.19	3.62
C_5PA	0.51	0.40
C_5PA	1.00	1.09
C_5PA	4.37	3.88
C_8PA	0.29	0.18
C_8PA	0.48	0.41
C_8PA	0.98	1.05
C_8PA	1.08	1.09
C_8PA	1.90	1.84
C_8PA	2.15	1.97
C_8PA	3.85	3.52
C_8PA	4.30	3.99
C_8PA	5.76	6.07
DEPA	0.55	0.44
DEPA	0.94	0.71
DEPA	1.64	1.13
DEPA	4.68	3.02
DEPA	5.27	3.86
DEPA	5.54	4.16
CAPA	0.49	0.53
CAPA	0.98	0.99
CAPA	1.95	2.03
CAPA	3.89	2.59
CAPA	4.84	2.75

6. Colloidal stability

The evolution of the solution structure has been characterized as a function of time. This has been achieved with DLS measurements during 6 days, for two NP concentrations, 1 wt % (as in zetametry) and 0.1 wt % (as with scattering), for various grafting densities of C_3PA and C_8PA. The result for R^{DLS} is shown in Fig. S4.

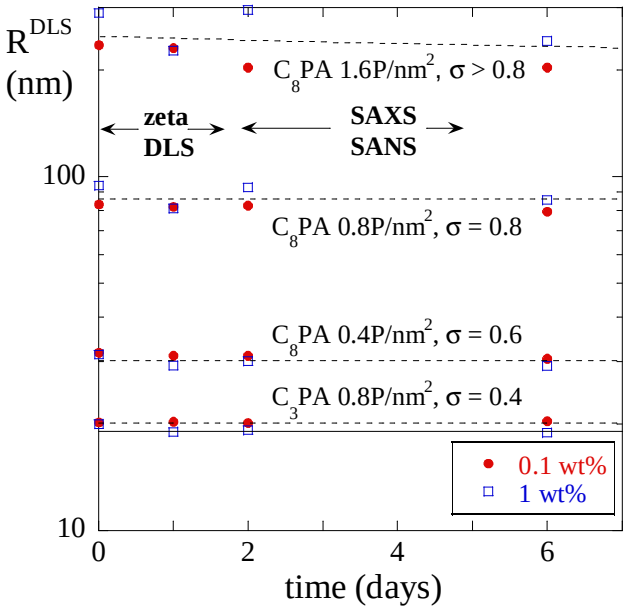

Fig. S4 Stability of dilute suspensions of NPs (1 wt % and 0.1 wt %) observed by DLS. The apparent hydrodynamic radius deduced from a cumulant analysis is plotted as a function of time. The solid line stands for R^{DLS} of the bare NPs. The legend indicates the different grafts with their grafting density ρ, and polydispersity σ. The arrows refer to the time windows of various characterizations.

We have also checked the influence of shaking the sample as usually done just before the experiments. It was found that this led to minor modifications of the order of 10% in R^{DLS} only for the highest grafting densities of C_8PA, which also showed some sedimentation by visual inspection. The more concentrated solutions – 5 wt % and 1 wt % as compared to 0.1 wt % – were found to be as stable in time as the dilute ones, with similar R^{DLS}.

7. Changes in interactions

For all SAXS measurements, the scattered intensities have been normalized to the high-q intensity of the bare NPs representing the form factor P(q) in order to compensate variations in capillary diameter and NP concentration induced by sedimentation.

7.1. CAPA

The data obtained for the particles modified with CAPA, carrying a carboxylic acid end-group, bring further insight for the interpretation of the results with respect to the influence of hydrophobicity and electrostatic charges. In DLS, CAPA-grafting was found to make the system more prone to aggregation. Reflecting structure on a more local scale, the scattered intensities are compared in Fig. S5, for increasing CAPA-grafting densities. In the inset, the corresponding structure factors are shown.

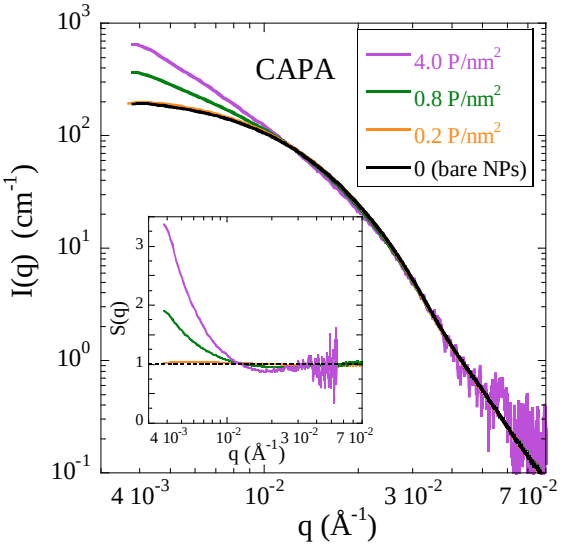

Fig. S5 Scattered intensity from SAXS for NPs grafted with CAPA at 0.2 vol % in water. The grafting densities are 0 (bare), 0.2 and 0.8 P/nm^2. For comparison, the strongly aggregated case of the much higher grafting density of 4 P/nm^2 is also shown, see text for details. Structure factors are shown in the inset.

The series of intensities follows the grafting density. At the lowest grafting density, ρ = 0.2 P/nm^2, the result is superimposed to the form factor scattering, indicating absence of interactions. For ρ = 0.8 P/nm^2, the low-q upturn below 0.01 Å^{-1} leads to S(q) approaching two in our q-window, and the local structure at high q stays identical. The highest grafting density of 4.0 P/nm^2, which according to Fig. 3(b) corresponds to strongly aggregated

samples, is shown for comparison. The scattering stems from the (even more dilute) supernatant, which explains the important noise. Nonetheless, the strong upturn characteristic for the interactions between the remaining NPs is in line with the previous observations.

References

1 P. Lindner, *Neutrons, X-ray and Light Scattering*, North Holland, Elsevier, 2002.

2 S. Brunauer, P. H. Emmett and E. Teller, *Journal of the American Chemical Society*, 1938, **60**, 309-319.

3 V. Verdinelli, P. V. Messina, P. C. Schulz and B. Vuano, *Colloids and Surfaces A: Physicochemical and Engineering Aspects*, 2008, **316**, 131-135.

4 J. T. Davies, *A quantitative kinetic theory of emulsion type I. Physical chemistry of the emulsifying agent. Gas/Liquid and Liquid/Liquid Interfaces. Proceedings of the International Congress of Surface Activity*, Butterworths, London, 1957.

5 B. O. Acton, G. G. Ting, P. J. Shamberger, F. S. Ohuchi, H. Ma and A. K. Y. Jen, *ACS Applied Materials & Interfaces*, 2010, **2**, 511-520.